International Journal of Engineering, Mathematical and Physical Sciences
ISSN: 2517-9934
Vol:5, No:8, 2011

Pulsating flow of an incompressible couple stress fluid between permeable beds

T.K.V. Iyengar and Punnamchandar Bitla

Abstract—The paper deals with the pulsating flow of an incompressible couple stress fluid between permeable beds. The couple stress fluid is injected into the channel from the lower permeable bed with a certain velocity and is sucked into the upper permeable bed with the same velocity. The flow between the permeable beds is assumed to be governed by couple stress fluid flow equations of V. K. Stokes and that in the permeable regions by Darcy's law. The equations are solved analytically and the expressions for velocity and volume flux are obtained. The effects of the material parameters are studied numerically and the results are presented through graphs.

Keywords—Pulsating flow, couple stress fluid, permeable beds, mass flux, shear stress

I. Introduction

THE importance of the study of the pulsatile flow in a channel or a porous pipe is too well known to be elaborated. It has biological applications in relation to hemodynamics [1], [2], industrial applications in relation to heat exchange efficiency, applications in natural systems like circulatory systems, respiratory systems, vascular diseases, in engineering systems like reciprocating pumps, IC engines, combustors and applications in MEMS micro fluidic engineering applications [3].

The terms 'pulsatile','oscillatory' or 'unsteady' are generally used in the literature to describe the flows in which velocity or pressure or both depend on time. Oscillatory flow is a periodic flow that oscillates around a zero value. Pulsatile flow is a periodic flow that oscillates around a mean value not equal to zero, i.e., it is a steady flow on which is superposed an oscillatory flow. Wang [4] studied the pulsatile flow of a viscous fluid in a porous channel. Vajravelu et al. [5] studied the pulsatile flow of a viscous fluid between permeable beds.

The boundary conditions for the flow through porous beds need special attention. Generally the no-slip condition is valid on the boundary when a fluid flows between impermeable surfaces. But when it flows between permeable surfaces, the no-slip condition is no longer valid since there will be a migration of fluid, tangential to the boundary within the permeable surfaces. The velocity within the permeable beds will be different from the velocity of the fluid in the channel and we have to match the two velocities at the interface. Beavers and Joseph in [6] based on their experimental investigations proposed that the slip velocity is related to the tangential stress. Then the Poiseuille velocity in the channel and the Darcy's velocity in the porous wall can be coupled through the following equation (known as Beavers and Joseph (BJ) condition)

$$\left(\frac{du}{dy}\right)_{y=0+} = \frac{\alpha}{\sqrt{k}}\,(u_s - D) \tag{1}$$

Here u_s is the slip velocity, i.e., the local averaged tangential velocity just outside the porous medium, $D(=-\frac{k}{\mu}\frac{\partial p}{\partial x})$ is the velocity inside the porous bed, given by Darcy's law, k is the permeability of the porous medium and the slip coefficient α is a dimensionless constant depending on the geometry of the interstices.

To the extent the present authors have surveyed the pulsatile flow of an incompressible couple stress fluid between two permeable beds has not been studied so far. The couple stress fluid theory is one of the fluid theories that has arisen to explain the deviation in the behavior of real fluids with that of Newtonian fluids. It is the simplest theory that shows all the important features and effects of couple stresses in a fluid medium and the basic equations describing a couple stress fluid flow are similar to the Navier Stokes equations, however, with the order of the differential equations increased by two. Stokes introduced this theory in 1966 [7] and since then there has been considerable interest regarding the study of various problems in fluid dynamics in the context of couple stress fluid flow. Stokes has written an exemplary treatise on theories of fluids with microstructure in which he has presented a detailed account of couple stress fluids [8]. Lakshmana Rao and Iyengar made analytical and computational studies of some axisymmetric couple stress fluid flows [9]. Several of the couple stress fluid flow problems studied upto 1984 can be seen in [8]. Srivastava studied the flow of a couple stress fluid through stenotic blood vessels [10]. He also studied the peristaltic transport of a couple stress fluid [11]. Naduvinamani et al. studied a number of problems with couple stress fluid between porous journal bearings and porous rectangular plates [12]–[14]. Devakar and Iyengar studied Stokes Problems for an incompressible couple stress fluid [15] and the run up flow between parallel plates [16]. Radhika and Iyengar [17] studied the Stokes flow of an incompressible couple stress fluid past a porous spheriodal shell.

In this paper, we study the couple stress fluid flow between two permeable beds. The fluid is driven by an unsteady pressure gradient. The flow through the permeable beds is assumed to be governed by Darcy's law and the flow between permeable beds by couple stress fluid flow equations of Stokes. The equations are solved analytically and the expressions for velocity and mass flux are obtained. The numerical results are presented and discussed through graphs. We observe that our

T.K.V. Iyengar, Department of Mathematics, National Institute of Technology, Warangal-506004, A.P., India. e-mail: (iyengar.tkv@gmail.com).
Punnamchandar Bitla, Department of Mathematics, National Institute of Technology, Warangal-506004, A.P., India. e-mail:(punnam.nitw@gmail.com)

results are in good agreement with those obtained by Vajravelu et al. [5] in the respective special cases considered by them.

Nomenclature :

x, y	Cartesian co-ordinates
u	Velocity component in x-direction
$\bar{u}(y)$	Steady velocity component
$\tilde{u}(y,t)$	Unsteady velocity component
V	Suction/injection velocity
h	Width of the channel
k_1	Permeability of the lower bed
k_2	Permeability of the upper bed
σ_1	$(= h/\sqrt{k_1})$ dimensionless parameter
σ_2	$(= h/\sqrt{k_2})$ dimensionless parameter
u_{B_1}	Slip velocity at the lower bed
u_{B_2}	Slip velocity at the upper bed
Q_1	$-(k_1/\mu)(\partial p/\partial x)$ Darcy's velocity in the lower bed
Q_2	$-(k_2/\mu)(\partial p/\partial x)$ Darcy's velocity in the upper bed
Q	Mass flow
p	Pressure
ρ	Density
ω	Frequency
μ	Coefficient of viscosity
η	Coefficient of couple stress viscosity
α	Slip parameter
β	Couple stress parameter(=$h^2\mu/\eta$)
τ	Shear stress
ν	Kinematic viscosity
R	Reynolds number
N	Frequency parameter
σ	Porosity parameter

II. Mathematical Formulation

We consider the pulsatile flow an incompressible couple stress fluid between two permeable beds. The fluid is injected into the channel from the lower permeable bed with a velocity V and is sucked into the upper permeable bed with the same velocity. The permeabilities of lower and upper beds are k_1 and k_2 respectively. The flow in upper and lower permeable beds is assumed to be governed by Darcy's law. The flow between the permeable beds is assumed to be governed by couple stress fluid flow equations of V. K. Stokes [8].

Let the x-axis be taken along the interface and the y-axis perpendicular to it. Let $y = 0$ and $y = h$ represent the interfaces of the permeable beds under consideration (see fig.1).

The following assumptions are made in the analysis of the problem:
(a) the permeable beds are homogeneous;
(b) the flow is laminar and fully developed;
(c) the fluid is driven by an unsteady pressure gradient,

$$\frac{1}{\rho}\frac{\partial p}{\partial x} = A + Be^{i\omega t} \tag{2}$$

where A and B are constants and ω is the frequency.

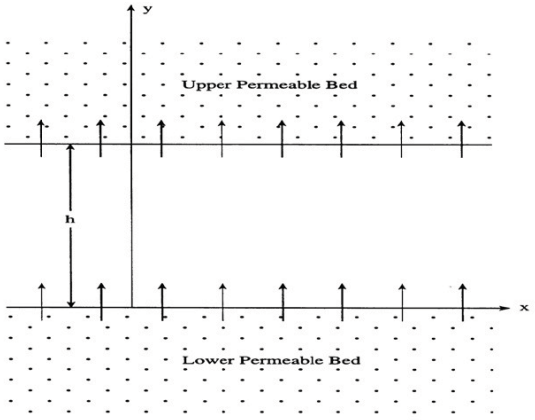

Fig. 1. Flow Diagram

The field equations describing a couple stress fluid flow are [8]

$$\frac{\partial \rho}{\partial t} + div(\rho \bar{q}) = 0 \tag{3}$$

$$\rho\frac{d\bar{q}}{dt} = \rho\bar{f} + \frac{1}{2}curl(\rho\bar{c}) - gradp - \mu curl(curl\bar{q}) - \eta curl(curl(curl(curl\bar{q}))) + (\lambda + 2\mu)grad(div\bar{q}) \tag{4}$$

where ρ is the density of the fluid, $\bar{q}$ is the velocity vector, p is the fluid pressure and $\bar{f}$, $\bar{c}$ are the body force per unit mass and body couple per unit mass respectively. The quantities λ and μ are the viscosity coefficients and η, η' are the couple stress viscosity coefficients satisfying the constraints

$$\mu \geq 0,\ 3\lambda + 2\mu \geq 0,\ \eta \geq 0,\ |\eta'| \leq \eta \tag{5}$$

There is a length parameter $l = \sqrt{\frac{\eta}{\mu}}$ which is a characteristic measure of the polarity of the couple stress fluid and this parameter is identically zero in the case of non polar fluids.

Under the assumptions made, we have $\bar{q} = (u(y,t), V, 0)$. In the absence of body forces and body couples, the governing equations of the problem are given by

$$\frac{\partial u}{\partial x} + \frac{\partial v}{\partial y} = 0 \tag{6}$$

$$\rho\left(\frac{\partial u}{\partial t} + V\frac{\partial u}{\partial y}\right) = -\frac{\partial p}{\partial x} + \mu\frac{\partial^2 u}{\partial y^2} - \eta\frac{\partial^4 u}{\partial y^4} \tag{7}$$

$$0 = \frac{\partial p}{\partial y} \tag{8}$$

Herein the velocity component $u(y,t)$ is to satisfy the conditions

$$\left.\begin{array}{lll} u = u_{B_1} & \text{at} & y = 0 \\ u = u_{B_2} & \text{at} & y = h \end{array}\right\} \text{(Slip velocities on the boundary)} \tag{9}$$

$$\left.\begin{array}{lll} \dfrac{\partial u}{\partial y} = \dfrac{\alpha}{\sqrt{k_1}}(u_{B_1} - Q_1) & \text{at} & y = 0 \\ \dfrac{\partial u}{\partial y} = -\dfrac{\alpha}{\sqrt{k_2}}(u_{B_2} - Q_2) & \text{at} & y = h \end{array}\right\} \text{(BJ conditions)} \tag{10}$$

$$\left.\begin{array}{lll}\dfrac{\partial^2 u}{\partial y^2}=0 & \text{at} & y=0\\ \dfrac{\partial^2 u}{\partial y^2}=0 & \text{at} & y=h\end{array}\right\}\ \text{(Vanishing of couple stresses)} \tag{11}$$

Stokes has proposed two types of boundary conditions (A) and (B) respectively and the vanishing of couple stresses on the boundary is referred to as condition (A) [8]. This condition (A) is adopted here as this is appropriate in the present context.

Let us assume that

$$u(y,t)=\bar{u}+\tilde{u} \tag{12}$$

where $\bar{u}$ and $\tilde{u}$ represent steady and unsteady parts of the velocity component respectively. We proceed to determine the steady part $\bar{u}(y)$ and later the unsteady part $\tilde{u}(y,t)$. Using (12) in equations (9)-(11), we get the respective governing equations and boundary conditions to be satisfied by $\bar{u}$ and $\tilde{u}$.

A. Determination of the Steady Part $\bar{u}$

The governing equations and boundary conditions that lead to the determination of $\bar{u}(y)$ are given by

$$\frac{\partial \bar{u}}{\partial x}=0 \tag{13}$$

$$\rho V\frac{\partial \bar{u}}{\partial y}=-\rho A+\mu\frac{\partial^2 \bar{u}}{\partial y^2}-\eta\frac{\partial^4 \bar{u}}{\partial y^4} \tag{14}$$

The boundary conditions to be satisfied by $\bar{u}(y)$ are

$$\left.\begin{array}{lll}\bar{u}=\bar{u}_{B_1} & \text{at} & y=0\\ \bar{u}=\bar{u}_{B_2} & \text{at} & y=h\end{array}\right\}\ \text{(Slip velocities on the boundary)} \tag{15}$$

$$\left.\begin{array}{l}\dfrac{d\bar{u}}{dy}=\dfrac{\alpha}{\sqrt{k_1}}(\bar{u}_{B_1}-\bar{Q}_1)\quad \text{at}\quad y=0\\ \dfrac{d\bar{u}}{dy}=-\dfrac{\alpha}{\sqrt{k_2}}(\bar{u}_{B_2}-\bar{Q}_2)\ \text{at}\quad y=h\end{array}\right\}\ \text{(BJ conditions)} \tag{16}$$

$$\left.\begin{array}{lll}\dfrac{d^2\bar{u}}{dy^2}=0 & \text{at} & y=0\\ \dfrac{d^2\bar{u}}{dy^2}=0 & \text{at} & y=h\end{array}\right\}\ \text{(Vanishing of couple stresses)} \tag{17}$$

where

$$\bar{Q}_1=-\frac{k_1\rho A}{\mu},\quad \bar{Q}_2=-\frac{k_2\rho A}{\mu} \tag{18}$$

B. Determination of the Unsteady Part $\tilde{u}$

The governing equations and the boundary conditions that lead to the determination of $\tilde{u}(y,t)$ are given by

$$\frac{\partial \tilde{u}}{\partial x} = 0 \tag{19}$$

$$\rho\left(\frac{\partial \tilde{u}}{\partial t}+V\frac{\partial \tilde{u}}{\partial y}\right) = -\rho Be^{i\omega t}+\mu\frac{\partial^2 \tilde{u}}{\partial y^2}-\eta\frac{\partial^4 \tilde{u}}{\partial y^4} \tag{20}$$

The boundary conditions are

$$\left.\begin{array}{lll}\tilde{u}=\tilde{u}_{B_1} & \text{at} & y=0\\ \tilde{u}=\tilde{u}_{B_2} & \text{at} & y=h\end{array}\right\}\ \text{(Slip velocities on the boundary)} \tag{21}$$

$$\left.\begin{array}{l}\dfrac{\partial \tilde{u}}{\partial y}=\dfrac{\alpha}{\sqrt{k_1}}(\tilde{u}_{B_1}-\tilde{Q}_1)\quad \text{at}\quad y=0\\ \dfrac{\partial \tilde{u}}{\partial y}=-\dfrac{\alpha}{\sqrt{k_2}}(\tilde{u}_{B_2}-\tilde{Q}_2)\ \text{at}\quad y=h\end{array}\right\}\ \text{(BJ conditions)} \tag{22}$$

$$\left.\begin{array}{lll}\dfrac{\partial^2 \tilde{u}}{\partial y^2}=0 & \text{at} & y=0\\ \dfrac{\partial^2 \tilde{u}}{\partial y^2}=0 & \text{at} & y=h\end{array}\right\}\ \text{(Vanishing of couple stresses)} \tag{23}$$

where

$$\tilde{Q}_1=-\frac{k_1\rho Be^{i\omega t}}{\mu},\quad \tilde{Q}_2=-\frac{k_2\rho Be^{i\omega t}}{\mu} \tag{24}$$

III. Non-dimensionalization of the Flow Quantities

The following non-dimensional quantities are introduced to make the basic equations and the boundary conditions dimensionless.

Steady Part:

$$\bar{u}^*=\frac{\bar{u}}{(A_1h/V)},\quad \bar{u}^*_{B_1}=\frac{\bar{u}_{B_1}}{(A_1h/V)},\quad \bar{u}^*_{B_2}=\frac{\bar{u}_{B_2}}{(A_1h/V)},$$
$$\bar{Q}^*_1=\frac{\bar{Q}_1}{(A_1h/V)},\quad \bar{Q}^*_2=\frac{\bar{Q}_2}{(A_1h/V)},\quad y^*=\frac{y}{h}$$
$$\text{where}\ \ A_1=-A \tag{25}$$

Unsteady Part:

$$\tilde{u}^*=\frac{\tilde{u}}{(h^2B_1/\upsilon)},\quad \tilde{u}^*_{B_1}=\frac{\tilde{u}_{B_1}}{(h^2B_1/\upsilon)},\quad \tilde{u}^*_{B_2}=\frac{\tilde{u}_{B_2}}{(h^2B_1/\upsilon)},$$
$$\tilde{Q}^*_1=\frac{\tilde{Q}_1}{(h^2B_1/\upsilon)},\quad \tilde{Q}^*_2=\frac{\tilde{Q}_2}{(h^2B_1/\upsilon)},\quad t^*=\frac{t}{(h^2/\upsilon)},$$
$$\omega^*=\frac{\omega}{(\upsilon/h^2)},\quad y^*=\frac{y}{h}\ \ \text{where}\ \ \ B_1=-B \tag{26}$$

In view of the dimensionless quantities, equations (13) to (17) and (19) to (23) take the following from as in (27) to (31) and (33) to (38) respectively as given below (dropping the asterisks$(*)$).

A. Steady Part :

The equations and boundary conditions governing the non-dimensionalized steady part $\bar{u}(y)$ are given by

$$\frac{d\bar{u}}{dx}=0 \tag{27}$$

$$\frac{1}{\beta^2}\frac{d^4\bar{u}}{dy^4}-\frac{d^2\bar{u}}{dy^2}+R\frac{d\bar{u}}{dy}=R \tag{28}$$

$$\left.\begin{array}{lll}\bar{u}=\bar{u}_{B_1} & \text{at} & y=0\\ \bar{u}=\bar{u}_{B_2} & \text{at} & y=1\end{array}\right\}\ \text{(Slip velocities on the boundary)} \tag{29}$$

$$\left.\begin{array}{l} \dfrac{d\bar{u}}{dy} = \alpha\sigma_1\left(\bar{u}_{B_1} - \dfrac{R}{\sigma_1^2}\right) \quad \text{at} \quad y=0 \\ \dfrac{d\bar{u}}{dy} = -\alpha\sigma_2\left(\bar{u}_{B_2} - \dfrac{R}{\sigma_2^2}\right) \text{at} \quad y=1 \end{array}\right\} \text{(BJ Conditions)} \tag{30}$$

$$\left.\begin{array}{l} \dfrac{d^2\bar{u}}{dy^2} = 0 \quad \text{at} \quad y=0 \\ \dfrac{d^2\bar{u}}{dy^2} = 0 \quad \text{at} \quad y=1 \end{array}\right\} \text{(Vanishing of couple stresses)} \tag{31}$$

where

$$R = \frac{\rho V h}{\mu},\ \sigma_1 = \frac{h}{\sqrt{k_1}},\ \sigma_2 = \frac{h}{\sqrt{k_2}},\ \beta^2 = \frac{h^2\mu}{\eta} \tag{32}$$

B. Unsteady Part

The non-dimensionalized equations governing $\tilde{u}(y,t)$ are given by

$$\frac{d\tilde{u}}{dx} = 0 \tag{33}$$

$$\frac{1}{\beta^2}\frac{d^4\tilde{u}}{dy^4} - \frac{d^2\tilde{u}}{dy^2} + R\frac{d\tilde{u}}{dy} + \frac{d\tilde{u}}{dt} = e^{i\omega t} \tag{34}$$

Introducing $\tilde{u} = \tilde{f}(y)e^{i\omega t}$, the equation (35) results in

$$\frac{1}{\beta^2}\frac{d^4\tilde{f}}{dy^4} - \frac{d^2\tilde{f}}{dy^2} + R\frac{d\tilde{f}}{dy} + i\omega\tilde{f} = 1 \tag{35}$$

and using $\tilde{u}_{B_1} = \tilde{f}_1(y)e^{i\omega t}, \tilde{u}_{B_2} = \tilde{f}_2(y)e^{i\omega t}$ the boundary conditions (21) to (23) become

$$\left.\begin{array}{l} \tilde{f} = \tilde{f}_1 \quad \text{at} \quad y=0 \\ \tilde{f} = \tilde{f}_2 \quad \text{at} \quad y=1 \end{array}\right\} \text{(Slip velocities on the boundary)} \tag{36}$$

$$\left.\begin{array}{l} \dfrac{d\tilde{f}}{dy} = \alpha\sigma_1\left(\tilde{f}_1 - \dfrac{1}{\sigma_1^2}\right) \quad \text{at} \quad y=0 \\ \dfrac{d\tilde{f}}{dy} = -\alpha\sigma_2\left(\tilde{f}_2 - \dfrac{1}{\sigma_2^2}\right) \text{at} \quad y=1 \end{array}\right\} \text{(BJ conditions)} \tag{37}$$

$$\left.\begin{array}{l} \dfrac{d^2\tilde{f}}{dy^2} = 0 \quad \text{at} \quad y=0 \\ \dfrac{d^2\tilde{f}}{dy^2} = 0 \quad \text{at} \quad y=1 \end{array}\right\} \text{(Vanishing of couple stresses)} \tag{38}$$

where

$$R = \frac{\rho V h}{\mu},\ \sigma_1 = \frac{h}{\sqrt{k_1}},\ \sigma_2 = \frac{h}{\sqrt{k_2}},\ \beta^2 = \frac{h^2\mu}{\eta} \tag{39}$$

IV. Solution of the Problem

A. Steady Part

Solving Eq(28) subject to the conditions (Eqs.(29)-(31)), we get the velocity field as

$$\bar{u} = C_1 + C_2 e^{\lambda_2 y} + C_3 e^{\lambda_3 y} + C_4 e^{\lambda_4 y} + y \tag{40}$$

where

$$\lambda_2 = (\beta^2/a_1 + a_1/3)$$

$$\lambda_{3,4} = \left(-\lambda_2 \pm i\sqrt{3}(\beta^2/a_1 - a_1/3)\right)/2$$

$$a_1 = \sqrt[3]{3\beta^2\left(-9R + \sqrt{81R^2 - 12\beta^2}\right)/2}$$

and

$$C_1 = \frac{S}{\alpha\Delta_s}(E_{23} - E_{24} + E_{34}) + \bar{u}_{B_2} - 1 \tag{41}$$

$$C_2 = -\frac{SE_{34}}{\Delta_s} \tag{42}$$

$$C_3 = \frac{SE_{24}}{\Delta_s} \tag{43}$$

$$C_4 = -\frac{SE_{23}}{\Delta_s} \tag{44}$$

and the slip velocities as

$$\bar{u}_{B_1} = \left(\frac{R\alpha + \sigma_1}{\alpha\sigma_1^2}\right) - \frac{S(E_{23}\lambda_4 - E_{24}\lambda_3 + E_{34}\lambda_2)}{\alpha^2\sigma_1\Delta_s} \tag{45}$$

$$\bar{u}_{B_2} = \left(\frac{R\alpha - \sigma_2}{\alpha\sigma_2^2}\right) + \frac{S(E_{23}\lambda_4 e^{\lambda_4} - E_{24}\lambda_3 e^{\lambda_3} + E_{34}\lambda_2 e^{\lambda_2})}{\alpha^2\sigma_2\Delta_s} \tag{46}$$

where

$$\Delta_s = (E_{23}F_4 - E_{24}F_3 + E_{34}F_2) \tag{47}$$

$$F_i = (\lambda_i - \alpha\sigma_1)\sigma_2 + e^{\lambda_i}\sigma_1(\lambda_i + \alpha\sigma_2) \quad \text{for } i = 2,3,4 \tag{48}$$

$$E_{ij} = (e^{\lambda_i} - e^{\lambda_j})\lambda_i^2\lambda_j^2 \quad \text{for} \quad i,\ j = 2,3,4 \quad (i<j) \tag{49}$$

$$S = \sigma_1(1 - \frac{R\alpha}{\sigma_2}) + \sigma_2(1 + \frac{R\alpha}{\sigma_1}) + \alpha\sigma_1\sigma_2 \tag{50}$$

B. Unsteady Part

Solving Eq(35) subject to the conditions (Eqs.(36)-(38)), we get the unsteady velocity field as

$$\tilde{u} = \tilde{f}(y)e^{i\omega t} \tag{51}$$

where

$$\tilde{f}(y) = C_5 e^{\lambda_5 y} + C_6 e^{\lambda_6 y} + C_7 e^{\lambda_7 y} + C_8 e^{\lambda_8 y} + \frac{1}{M_0} \tag{52}$$

$$\lambda_{5,6} = \left(+d \pm \sqrt{6\beta^2(1 - \sqrt{3}R/d) - d^2}\right)/(2\sqrt{3}) \tag{53}$$

$$\lambda_{7,8} = \left(-d \pm \sqrt{6\beta^2(1 + \sqrt{3}R/d) - d^2}\right)/(2\sqrt{3}) \tag{54}$$

with

$$d = \sqrt{2\beta^2 + \frac{a}{c} + c};\ c = \sqrt[3]{\frac{b + \sqrt{b^2 - 4a^3}}{2}}$$

$$b = \beta^4[27R^2 + 72M_0 - 2\beta^2];\ a = \beta^2[12M_0 + \beta^2]$$

$$M_0 = iN^2, \quad N^2 = \omega$$

and

$$C_5 = \frac{\alpha}{\Delta}[-E_{78}F_6 + E_{68}F_7 - E_{67}F_8] \tag{55}$$

$$C_6 = \frac{\alpha}{\Delta}[E_{78}F_5 - E_{58}F_7 + E_{57}F_8] \tag{56}$$

$$C_7 = \frac{\alpha}{\Delta}[-E_{68}F_5 + E_{58}F_6 - E_{56}F_8] \tag{57}$$

$$C_8 = \frac{\alpha}{\Delta}[E_{67}F_5 - E_{57}F_6 + E_{56}F_7] \tag{58}$$

The slip velocities are seen to be $\tilde{u}_{B_j} = \tilde{f}_j e^{i\omega t}$ for $j = 1, 2$ where

$$\tilde{f}_1 = \frac{[E_{78}G_{56} - E_{68}G_{57} + E_{67}G_{58} + E_{58}G_{67} - E_{57}G_{68} + E_{56}G_{78}]}{\Delta} \quad (59)$$

$$\tilde{f}_2 = \frac{[E_{78}S_{56} - E_{68}S_{57} + E_{67}S_{58} + E_{58}S_{67} - E_{57}S_{68} + E_{56}S_{78}]}{\Delta} \quad (60)$$

$$\Delta = M_0\sigma_1\sigma_2[-E_{78}E\lambda_{56} + E_{68}E\lambda_{57} - E_{67}E\lambda_{58} - E_{58}E\lambda_{67} + E_{57}E\lambda_{68} - E_{56}E\lambda_{78}] \quad (61)$$

$$F_i = (M_0 - \sigma_2^2)\sigma_1(\lambda_i - \alpha\sigma_1) + e^{\lambda_i}(M_0 - \sigma_1^2)\sigma_2(\lambda_i + \alpha\sigma_2) \quad \text{for } i = 5, 6, 7, 8 \quad (62)$$

$$E_{ij} = (e^{\lambda_i} - e^{\lambda_j})\lambda_i^2\lambda_j^2 \quad \text{for } i, j = 5, 6, 7, 8 \quad (i < j) \quad (63)$$

$$E\lambda_{ij} = e^{\lambda_i}(\lambda_i + \alpha\sigma_2)(\lambda_j - \alpha\sigma_1) - e^{\lambda_j}(\lambda_j + \alpha\sigma_2)(\lambda_i - \alpha\sigma_1) \quad \text{for } i, j = 5, 6, 7, 8 \quad (i < j) \quad (64)$$

$$G_{ij} = (M_0 - \sigma_2^2)(\lambda_i - \lambda_j)\alpha\sigma_1 + e^{\lambda_i}(\lambda_i + \alpha\sigma_2)(M_0\alpha - \lambda_j\sigma_1)\sigma_2 - e^{\lambda_j}(\lambda_j + \alpha\sigma_2)(M_0\alpha - \lambda_i\sigma_1)\sigma_2 \quad \text{for } i, j = 5, 6, 7, 8 \quad (i < j) \quad (65)$$

and

$$S_{ij} = e^{\lambda_i + \lambda_j}(M_0 - \sigma_1^2)(\lambda_i - \lambda_j)\alpha\sigma_2 + e^{\lambda_j}(\lambda_i - \alpha\sigma_1)(M_0\alpha + \lambda_j\sigma_2)\sigma_1 - e^{\lambda_i}(\lambda_j - \alpha\sigma_1)(M_0\alpha + \lambda_i\sigma_2)\sigma_1 \quad \text{for } i, j = 5, 6, 7, 8 \quad (i < j) \quad (66)$$

V. Deductions

Taking $k_1 = k_2 = k$ (i.e. $\sigma_1 = \sigma_2 = \sigma$) in Eqs. (40) to (50) and (51) to (66), we obtain the velocity field as follows

A. Steady Part

The steady part of the velocity is given by

$$\bar{u} = C_1 + C_2 e^{\lambda_2 y} + C_3 e^{\lambda_3 y} + C_4 e^{\lambda_4 y} + y \quad (67)$$

where

$$\lambda_2 = (\beta^2/a_1 + a_1/3)$$

$$\lambda_{3,4} = \left(-\lambda_2 \pm i\sqrt{3}(\beta^2/a_1 - a_1/3)\right)/2$$

$$a_1 = \sqrt[3]{3\beta^2\left(-9R + \sqrt{81R^2 - 12\beta^2}\right)/2}$$

and

$$C_1 = \frac{S}{\alpha\Delta_s}(E_{23} - E_{24} + E_{34}) + \bar{u}_{B_2} - 1 \quad (68)$$

$$C_2 = -\frac{SE_{34}}{\Delta_s} \quad (69)$$

$$C_3 = \frac{SE_{24}}{\Delta_s} \quad (70)$$

$$C_4 = -\frac{SE_{23}}{\Delta_s} \quad (71)$$

The slip velocities are seen to be

$$\bar{u}_{B_1} = \left(\frac{R\alpha + \sigma}{\alpha\sigma^2}\right) - \frac{S(E_{23}\lambda_4 - E_{24}\lambda_3 + E_{34}\lambda_2)}{\alpha^2\sigma\Delta_s} \quad (72)$$

$$\bar{u}_{B_2} = \left(\frac{R\alpha - \sigma}{\alpha\sigma^2}\right) + \frac{S(E_{23}\lambda_4 e^{\lambda_4} - E_{24}\lambda_3 e^{\lambda_3} + E_{34}\lambda_2 e^{\lambda_2})}{\alpha^2\sigma\Delta_s} \quad (73)$$

where

$$\Delta_s = (E_{23}F_4 - E_{24}F_3 + E_{34}F_2) \quad (74)$$

$$F_i = \sigma((\lambda_i - \alpha\sigma) + e^{\lambda_i}(\lambda_i + \alpha\sigma)) \quad \text{for } i = 2, 3, 4 \quad (75)$$

$$E_{ij} = (e^{\lambda_i} - e^{\lambda_j})\lambda_i^2\lambda_j^2 \quad \text{for } i, j = 2, 3, 4 \quad (i < j) \quad (76)$$

$$S = \sigma(2 + \alpha\sigma) \quad (77)$$

B. Unsteady Part

The unsteady part of the velocity is given by

$$\tilde{u} = \tilde{f}(y)e^{i\omega t} \quad (78)$$

where

$$\tilde{f}(y) = C_5 e^{\lambda_5 y} + C_6 e^{\lambda_6 y} + C_7 e^{\lambda_7 y} + C_8 e^{\lambda_8 y} + \frac{1}{M_0} \quad (79)$$

$$\lambda_{5,6} = \left(+d \pm \sqrt{6\beta^2(1 - \sqrt{3}R/d) - d^2}\right)/(2\sqrt{3}) \quad (80)$$

$$\lambda_{7,8} = \left(-d \pm \sqrt{6\beta^2(1 + \sqrt{3}R/d) - d^2}\right)/(2\sqrt{3}) \quad (81)$$

with

$$d = \sqrt{2\beta^2 + \frac{a}{c} + c}\,;\; c = \sqrt[3]{\frac{b + \sqrt{b^2 - 4a^3}}{2}}$$

$$b = \beta^4[27R^2 + 72M_0 - 2\beta^2]\,;\; a = \beta^2[12M_0 + \beta^2]$$

and

$$C_5 = \frac{\alpha}{\Delta}[-E_{78}F_6 + E_{68}F_7 - E_{67}F_8] \quad (82)$$

$$C_6 = \frac{\alpha}{\Delta}[E_{78}F_5 - E_{58}F_7 + E_{57}F_8] \quad (83)$$

$$C_7 = \frac{\alpha}{\Delta}[-E_{68}F_5 + E_{58}F_6 - E_{56}F_8] \quad (84)$$

$$C_8 = \frac{\alpha}{\Delta}[E_{67}F_5 - E_{57}F_6 + E_{56}F_7] \quad (85)$$

The slip velocities are seen to be $\tilde{u}_{B_j} = \tilde{f}_j e^{i\omega t}$ for $j = 1, 2$ where

$$\tilde{f}_1 = \frac{[E_{78}G_{56} - E_{68}G_{57} + E_{67}G_{58} + E_{58}G_{67} - E_{57}G_{68} + E_{56}G_{78}]}{\Delta} \quad (86)$$

$$\tilde{f}_2 = \frac{[E_{78}S_{56} - E_{68}S_{57} + E_{67}S_{58} + E_{58}S_{67} - E_{57}S_{68} + E_{56}S_{78}]}{\Delta} \quad (87)$$

$$\Delta = M_0\sigma^2[-E_{78}E\lambda_{56} + E_{68}E\lambda_{57} - E_{67}E\lambda_{58} - E_{58}E\lambda_{67} + E_{57}E\lambda_{68} - E_{56}E\lambda_{78}] \quad (88)$$

$$F_i = \sigma(M_0 - \sigma^2)[(\lambda_i - \alpha\sigma) + e^{\lambda_i}(\lambda_i + \alpha\sigma)] \quad \text{for } i = 5, 6, 7, 8 \quad (89)$$

$$E_{ij} = (e^{\lambda_i} - e^{\lambda_j})\lambda_i^2\lambda_j^2 \quad \text{for } i, j = 5, 6, 7, 8 \quad (i < j) \quad (90)$$

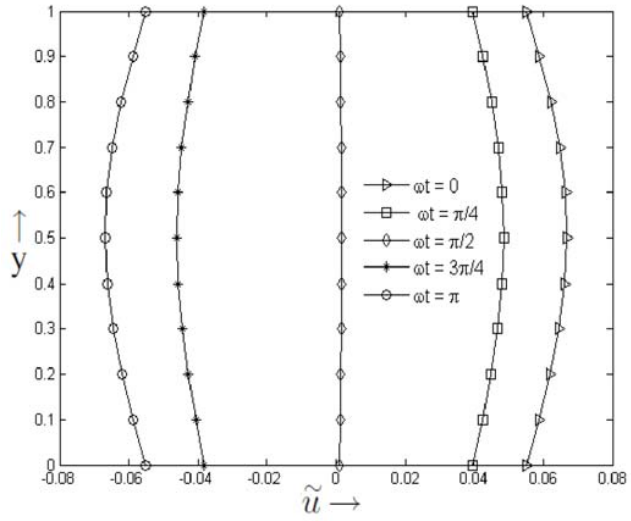

Fig. 2. Unsteady velocity profile $\tilde{u}(y,t)$ for $\sigma = 5,\ R = 2,\ \alpha = 0.5, N = 1,\ \beta = 1$

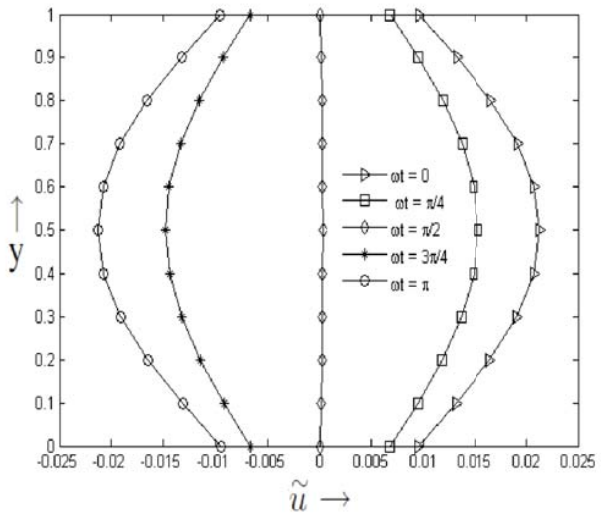

Fig. 3. Unsteady velocity profile $\tilde{u}(y,t)$ for $\sigma = 15,\ R = 2,\ \alpha = 0.5, N = 1,\ \beta = 1$

$$E\lambda_{ij} = e^{\lambda_i}(\lambda_i + \alpha\sigma)(\lambda_j - \alpha\sigma) - e^{\lambda_j}(\lambda_j + \alpha\sigma)(\lambda_i - \alpha\sigma) \quad \text{for} \quad i,\ j = 5,6,7,8\,(i < j) \quad (91)$$

$$G_{ij} = \sigma[(M_0 - \sigma^2)\alpha(\lambda_i - \lambda_j) + e^{\lambda_i}(\lambda_i + \alpha\sigma)(M_0\alpha - \lambda_j\sigma) - e^{\lambda_j}(\lambda_j + \alpha\sigma)(M_0\alpha - \lambda_i\sigma)] \quad \text{for} \quad i,\ j = 5,6,7,8\,(i < j) \quad (92)$$

and

$$S_{ij} = \sigma[e^{\lambda_i+\lambda_j}(M_0 - \sigma^2)\alpha(\lambda_i - \lambda_j) - e^{\lambda_i}(\lambda_j - \alpha\sigma)(M_0\alpha + \lambda_i\sigma) + e^{\lambda_j}(\lambda_i - \alpha\sigma)(M_0\alpha + \lambda_j\sigma)] \quad \text{for} \quad i,\ j = 5,6,7,8\,(i < j) \quad (93)$$

C. Mass Flow

The instantaneous mass flux Q is given by

$$Q = \left[\int_0^1 \tilde{f}(y)dy\right] e^{i\omega t} \quad (94)$$

where $\tilde{f}(y)$ is given by equation (52).

D. Shear Stress

Shear stress at the permeable walls can be obtained by using

$$\tilde{\tau} = \left(\frac{\partial \tilde{u}}{\partial y} - \frac{\partial^3 \tilde{u}}{\partial y^3}\right)_{\text{at } y=0,1} \quad (95)$$

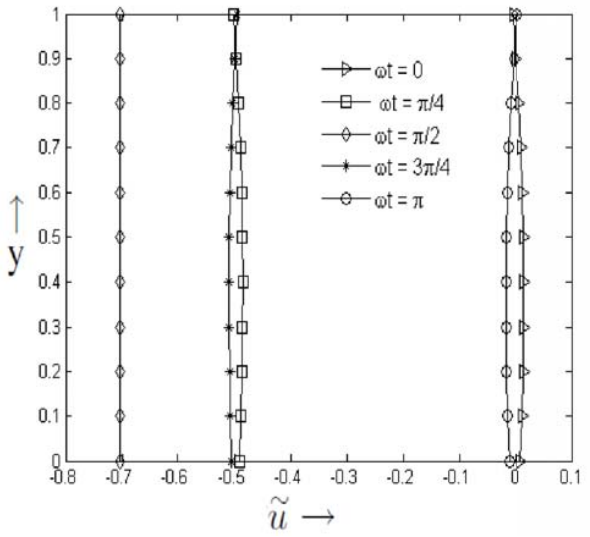

Fig. 4. Unsteady velocity profile $\tilde{u}(y,t)$ for $\sigma_1 = 5,\ \sigma_2 = 7,\ R = 6,\ \alpha = 0.5, N = 1,\ \beta = 1$

VI. Numerical Results and Discussion

The Figs.(2-4) display the variation of the unsteady velocity component with respect to the change in ωt. The values of ωt considered are 0, $\pi/2$, $\pi/4$, $3\pi/4$ and π. The velocity is decreasing as the porosity parameter σ is increasing. This can be seen in the Figs. 2 and 3. We have also displayed the variation in the unsteady velocity for different values of permeability parameters of the upper and lower beds for each of the values of ωt. These are displayed when $\sigma_1 = 5, \sigma_2 = 7, R = 6, N = 2, \alpha = 0.5, \beta = 1$. The variation is indicated in Fig.4.

Fig.5 shows the variation of the velocity component with respect to the couple stress parameter β. It is seen that as

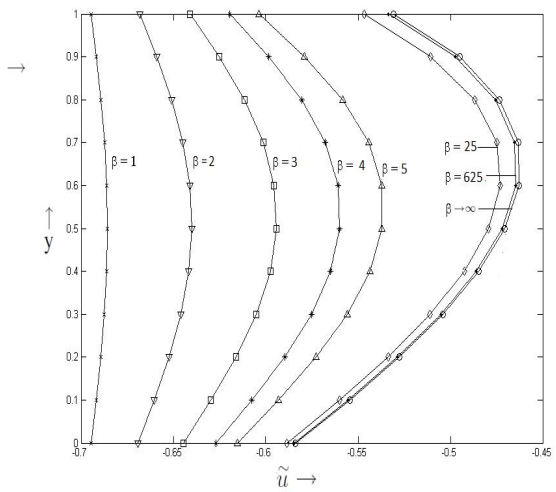

Fig. 5. Effect of β on $\tilde{u}(y,t)$ for $\alpha = 0.5,\ \sigma = 5, R = 2, N = 1, \omega t = \pi/4$

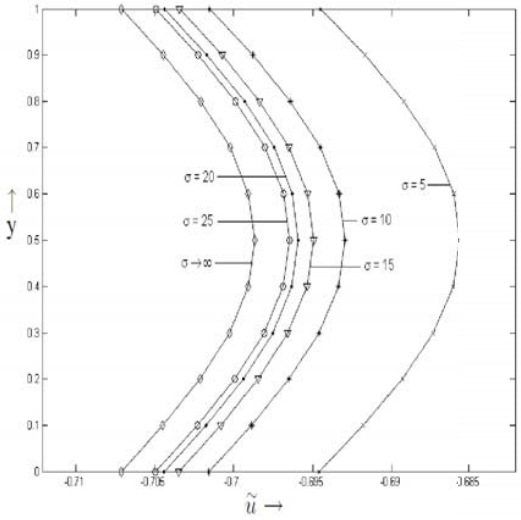

Fig. 6. Effect of σ on $\tilde{u}(y,t)$ for $\alpha = 0.5, R = 2, N = 1,\ \beta = 1, \omega t = \pi/4$

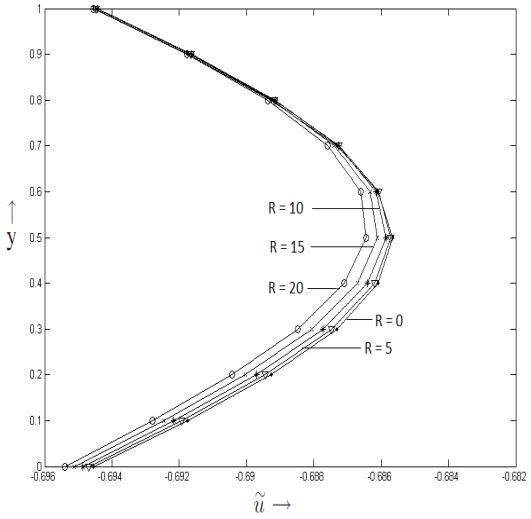

Fig. 7. Effect of R on $\tilde{u}(y,t)$ for $\alpha = 0.5, \sigma = 5, N = 1,\ \beta = 1, \omega t = \pi/4$

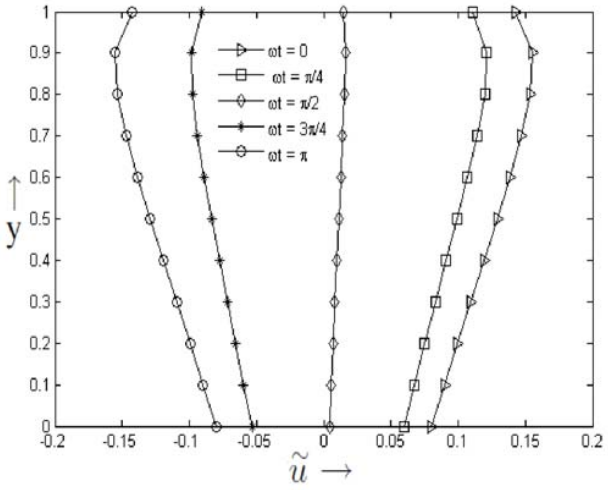

Fig. 8. Unsteady velocity profile $\tilde{u}(y,t)$ for $\alpha = 0.5,\ \sigma = 5,\ R = 10,\ N = 1,\ \beta \to \infty\,(\eta \to 0)$

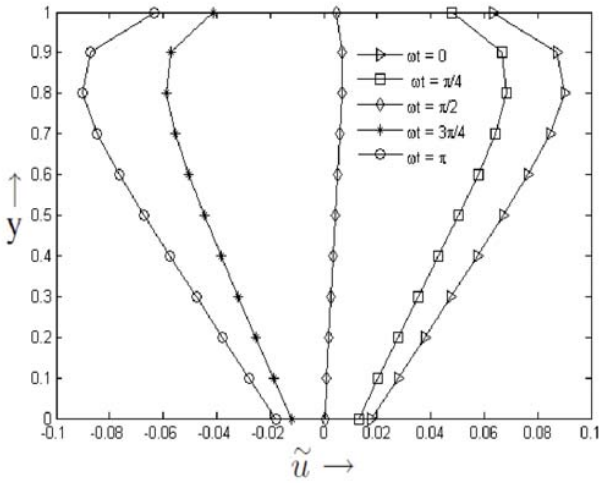

Fig. 9. Unsteady velocity profile $\tilde{u}(y,t)$ for $\alpha = 0.5,\ \sigma = 15,\ R = 10,\ N = 1,\ \beta \to \infty\,(\eta \to 0)$

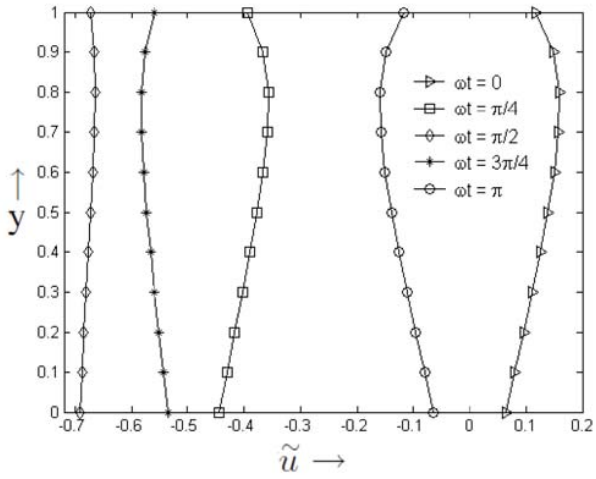

Fig. 10. Unsteady velocity profile $\tilde{u}(y,t)$ for $\sigma_1 = 5,\ \sigma_2 = 7,\ R = 6,\ \alpha = 0.5, N = 1, \beta \to \infty\,(\eta \to 0)$

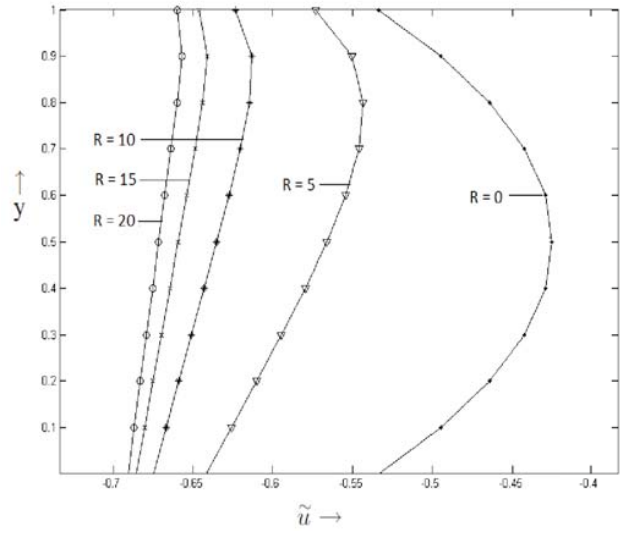

Fig. 11. Effect of R on $\tilde{u}(y,t)$ for $\alpha = 0.5, \sigma = 5, N = 1, \omega t = \pi/4, \beta \to \infty\,(\eta \to 0)$

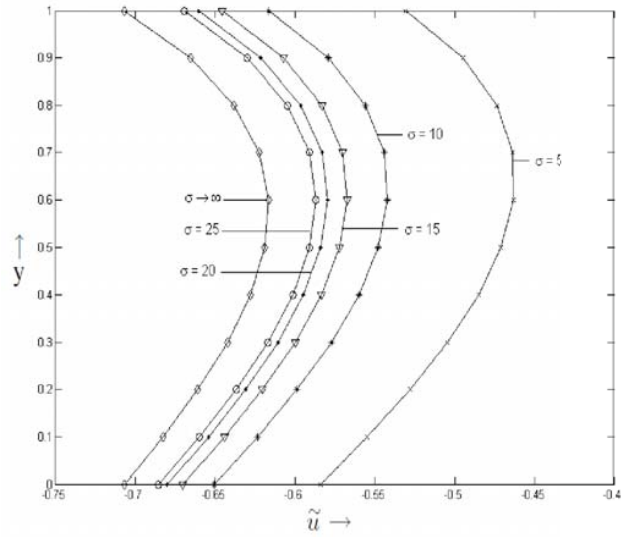

Fig. 12. Effect of σ on $\tilde{u}(y,t)$ for $\alpha = 0.5, R = 2, N = 1, \omega t = \pi/4$, $\beta \to \infty\,(\eta \to 0)$

β increases (i.e., as η decreases), the unsteady velocity component increases. As $\beta \to \infty$ (i.e., as $\eta \to 0$), the velocity component corresponds to non polar fluid.

The variation of the velocity component with respect to porosity parameter σ is depicted in Fig.6. As the porosity parameter is increasing (i.e., as k is decreasing), the unsteady velocity component is decreasing. As $\sigma \to \infty$ (i.e., as $k \to 0$), the velocity component corresponds to flow between rigid plates.

Variation of Reynolds number R for a fixed value of ωt seems to have less influence on the unsteady part of the velocity component. As R increases the velocity decreases. The decrease in velocity for each R is clearly visible for the region $y = 0$ to $y = 0.7$. As y varies from $y = 0.8$ to $y = 1$,

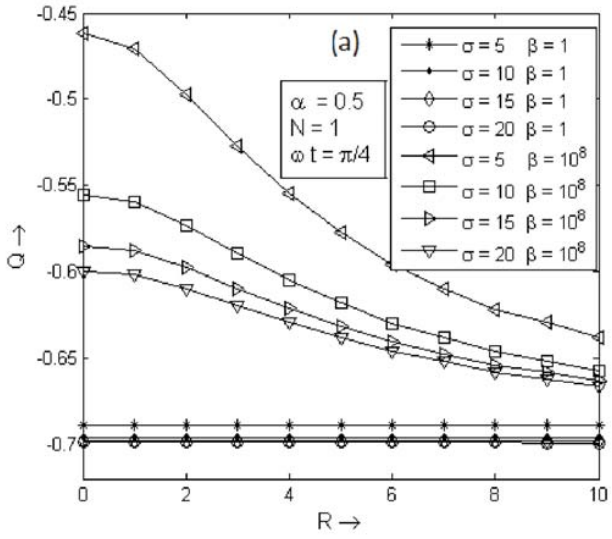

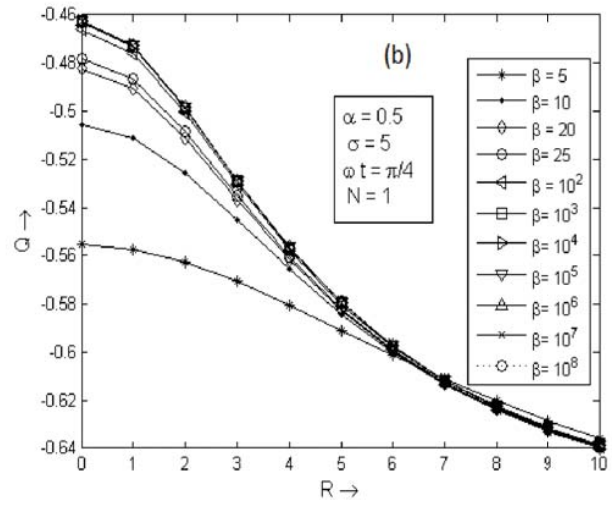

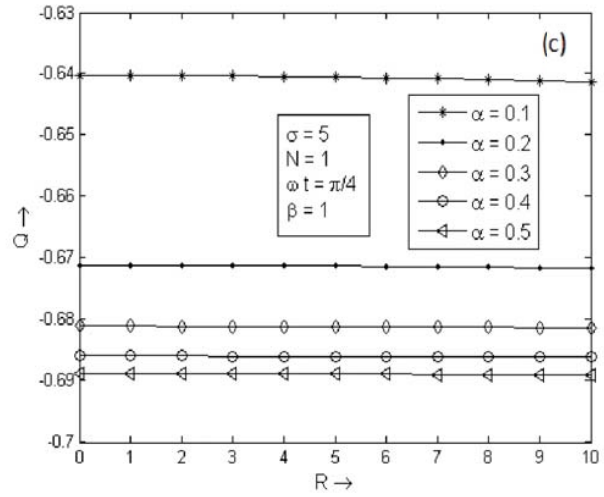

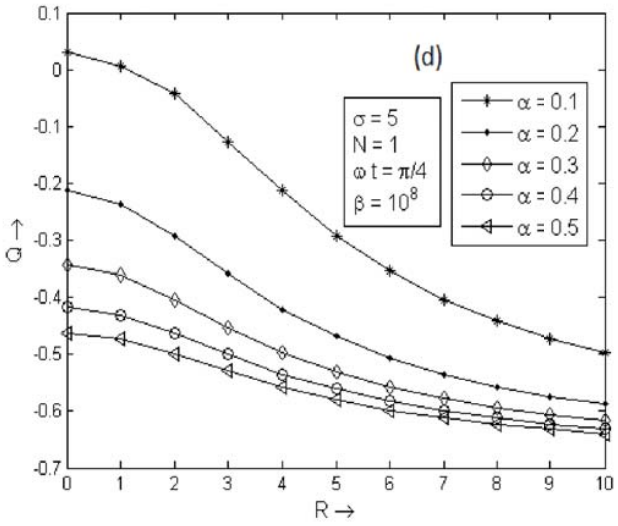

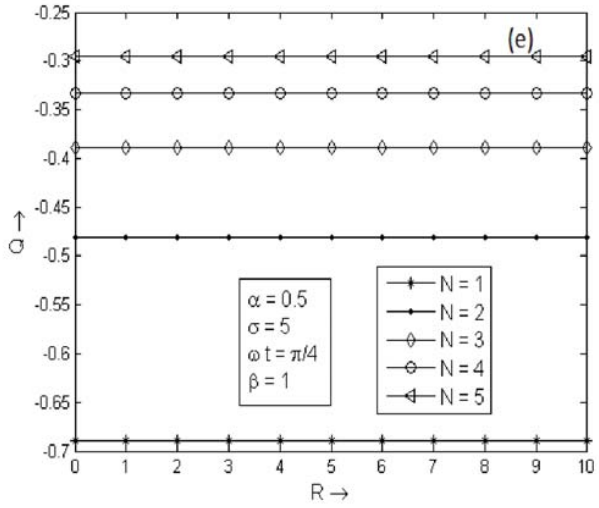

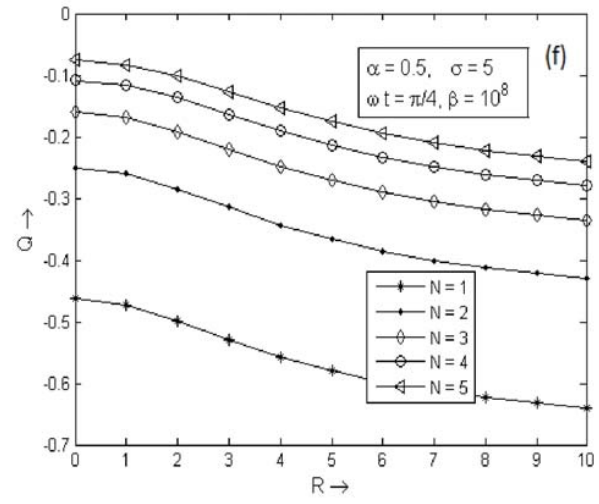

Fig. 13. Mass flux

TABLE I
VARIATION OF SHEAR STRESS WITH R AT THE INTERFACE OF LOWER PERMEABLE BED (LPB) AND UPPER PERMEABLE BED (UPB) ($\alpha = 0.5, \sigma = 5, N = 1, \beta = 1$)

$\lvert\tilde{\tau}\rvert$	R=0	R=2	R=4	R=6	R=8
$\omega t = 0$					
LPB	0.499269	0.484165	0.468864	0.453404	0.437821
UPB	0.499269	0.51414	0.528742	0.543043	0.557009
$\omega t = \pi/4$					
LPB	0.375199	0.363815	0.352278	0.340615	0.328856
UPB	0.375199	0.386401	0.397393	0.408151	0.418648
$\omega t = \pi/2$					
LPB	0.0313426	0.0303476	0.0293317	0.0282984	0.0272511
UPB	0.0313426	0.0323134	0.0332567	0.0341697	0.0350495
$\omega t = 3\pi/4$					
LPB	0.330874	0.320897	0.310796	0.300595	0.290317
UPB	0.330874	0.340703	0.350361	0.359828	0.369081

TABLE II
VARIATION OF SHEAR STRESS WITH α AT THE INTERFACE OF LOWER PERMEABLE BED (LPB) AND UPPER PERMEABLE BED (UPB) (R=5, M=2, N = 1, σ=5, β=1)

$\lvert\tilde{\tau}\rvert$	$\alpha = 0$	$\alpha = 0.2$	$\alpha = 0.4$	$\alpha = 0.6$	$\alpha = 0.8$
$\omega t = 0$					
LPB	0	0.459823	0.460947	0.461287	0.461459
UPB	0	0.534066	0.535614	0.536154	0.536449
$\omega t = \pi/4$					
LPB	0	0.352845	0.347538	0.345741	0.344842
UPB	0	0.409994	0.404	0.402011	0.401033
$\omega t = \pi/2$					
LPB	0	0.0391759	0.0305468	0.0276635	0.0262215
UPB	0	0.0457535	0.0357284	0.0323755	0.0306973
$\omega t = 3\pi/4$					
LPB	0	0.297442	0.304339	0.306618	0.307759
UPB	0	0.345289	0.353473	0.356225	0.35762

the velocity profiles are almost coinciding for each R (See Fig.7).

Figs.(8-10) show the variation of the unsteady velocity component, specifically, for the case of very large β which means that the fluid tends to be non polar. The values that we obtained for $\tilde{u}$ are coinciding with those obtained by Vajravelu et.al [5] in the case of non polar viscous fluid (Compare our Fig.8 with Fig.6 in [5]).

The effects of Reynolds number R and porosity parameter σ for non polar viscous fluid (i.e., as $\eta \to 0$) are depicted in Fig.11 and Fig.12 respectively. As Reynolds number R is increasing the velocity at any y is decreasing. For $R = 0$, the maximum velocity is attained exactly midway between the lower and upper permeable beds. As R increases, the maximum velocity is attained nearer to the upper permeable bed as can be seen from Fig.11. As the porosity parameter increases, we see that the velocity for any y decreases. In Fig.12 we have shown the velocity profile corresponding to $R = 2$. Here again the maximum velocity in each case occurs nearer to the upper plate.

TABLE III
VARIATION OF SHEAR STRESS WITH β AT THE INTERFACE OF LOWER PERMEABLE BED (LPB) AND UPPER PERMEABLE BED (UPB)
(α=0.5, R=5, N=1M=2, σ=5)

$\lvert\tilde{\tau}\rvert$	$\beta=1$	$\beta=3$	$\beta=5$	$\beta=7$	$\beta=9$
$\omega t=0$					
LPB	0.461152	1.38073	0.890743	0.5612	0.513366
UPB	0.535932	4.15251	8.96283	13.9658	19.1204
$\omega t=\pi/4$					
LPB	0.34646	1.09748	0.637805	0.282928	0.176557
UPB	0.402803	3.37977	7.50659	11.7563	16.108
$\omega t=\pi/2$					
LPB	0.028817	0.171341	0.0112483	0.161079	0.263676
UPB	0.0337172	0.627211	1.6531	2.66008	3.65974
$\omega t=3\pi/4$					
LPB	0.305707	0.855169	0.621897	0.510728	0.549451
UPB	0.35512	2.49276	5.16876	7.99437	10.9323

TABLE IV
VARIATION OF SHEAR STRESS WITH σ AT THE INTERFACE OF LOWER PERMEABLE BED (LPB) AND UPPER PERMEABLE BED (UPB)
($\alpha=0.5, R=5, M=2, N=1, \beta=1$)

$\lvert\tilde{\tau}\rvert$	$\sigma=1$	$\sigma=3$	$\sigma=5$	$\sigma=7$	$\sigma=9$
$\omega t=0$					
LPB	0.420379	0.459529	0.461152	0.461549	0.461718
UPB	0.487815	0.533847	0.535932	0.536515	0.536793
$\omega t=\pi/4$					
LPB	0.648137	0.371763	0.34646	0.338946	0.335655
UPB	0.752519	0.43206	0.402803	0.394153	0.390382
$\omega t=\pi/2$					
LPB	0.496225	0.0662234	0.028817	0.0177935	0.0129699
UPB	0.576407	0.0771782	0.0337172	0.0209013	0.0152901
$\omega t=3\pi/4$					
LPB	0.0536308	0.278109	0.305707	0.313782	0.317313
UPB	0.0626444	0.322913	0.35512	0.364594	0.368758

TABLE V
VARIATION OF SHEAR STRESS WITH N AT THE INTERFACE OF LOWER PERMEABLE BED (LPB) AND UPPER PERMEABLE BED (UPB)
(α=0.5, R=5, M=2, σ=10, β=1)

$\lvert\tilde{\tau}\rvert$	$N=1$	$N=2$	$N=3$	$N=4$	$N=5$
$\omega t=0$					
LPB	0.46177	0.461586	0.461402	0.461218	0.461034
UPB	0.536886	0.536666	0.536446	0.536227	0.536007
$\omega t=\pi/4$					
LPB	0.334653	0.337888	0.340339	0.342382	0.344165
UPB	0.389239	0.393057	0.395949	0.39836	0.400464
$\omega t=\pi/2$					
LPB	0.0115012	0.0162607	0.0199099	0.0229838	0.0256898
UPB	0.0135809	0.0192011	0.02351	0.0271396	0.0303348
$\omega t=3\pi/4$					
LPB	0.318388	0.314892	0.312182	0.309878	0.307835
UPB	0.370032	0.365903	0.362701	0.359979	0.357564

Finally, Fig.13 shows the variation in the mass flux with respect to change in various parameters. From Fig.13a, in both the cases for $\beta=1$ and 10^8, we observe that as σ increases the mass flux is seen to decrease. Further, for $\beta=10^8$, the decrease in the mass flux is more. As β increases through the values $5, 10, 20, 25$ and 100, the mass flux is seen to increase and after that further increase in β through the values $10^3, 10^4, 10^5, 10^6, 10^7, 10^8$ has no influence on the mass flux. As α increases the mass flux is seen to decrease in both the cases for $\beta=1$ and 10^8 and for fixed values of other parameters (see Figs. 13c and 13d). In Figs. 13e and 13f we observe that as N increases the mass flux seems to increase in both the cases for $\beta=1$ and 10^8.

The variation of shear stress is presented numerically through tables. From table I, we notice that for certain fixed values of α, σ, N and β, as the Reynolds number R increases for $\omega t=0, \pi/4, \pi/2$ and $3\pi/4$ at the lower bed the shear stress decreases while at the upper bed it increases. In table II, we have presented the variation of shear stress as α increases for a fixed set of values of the other parameters. At $\omega t=0$ and $3\pi/4$, it is seen that the shear stress at both the walls is increasing while at $\omega t=\pi/4$ and $\pi/2$, the shear stress at both the walls is decreasing.

Table III shows that at each ωt, as the couple stress parameter increases i.e., as the couple stress viscosity coefficient decreases, the shear stress at the upper wall has an increasing trend while at the lower wall no such trend is observed. In table IV, we notice that as the porosity parameter σ is increasing, for $\omega t=0$ and $3\pi/4$, it is seen that the shear stress at both the walls is increasing while for $\omega t=\pi/4$ and $\pi/2$, the shear stress at both the walls is decreasing. In table V, as the frequency parameter is increasing, for $\omega t=0$ and $3\pi/4$, it is seen that the shear stress at both the walls is decreasing while for $\omega t=\pi/4$ and $\pi/2$, the shear stress at both the walls is increasing.

In all cases, it is found that the shear stress at the lower wall is less than the shear stress at the upper wall.

VII. CONCLUSION

We have studied the pulsating flow of an incompressible couple stress fluid between permeable beds. It is observed that the presence of couple stresses results in a decrease in the velocity. Further, when the couple stresses are present, the Reynolds number seems to have no influence on the unsteady velocity component. This is in contrast with the disturbance we see in the absence of couple stresses. The results for Newtonian viscous fluid case are recoverable from our analysis.

REFERENCES

[1] D.N.Ku, D.P.Giddens, C.K. Zairns, S. Glagov, Pulsatile flow and atherosclerosis in human carotid bifurcation: positive correlation between plaque location and low and oscillating shear stress, Arteriosclerosis 5 (1985) 293–302.
[2] R.M.Nerem, M.J.Levesque, Hemodynamics and the arterial wall, Vasc. Disc. (1987) 295–317.
[3] F.Fedele, D.Hitt, R.D.Prabhu, Revisiting the stability of pulsatile pipe flow, European J. of Mech. — B/Fluids 24 (2005) 237–254.
[4] Y.C. Wang, Pulsatile flow in a porous channel, J. Appl. Mech. 38 (1971) 553–555.

[5] K. Vajravelu, K. Ramesh, S. Sreenadh, P.V. Arunachalam, Pulsatile flow between permeable beds, Int. J. Non-Linear Mech. 38 (2003) 999-1005
[6] G.S. Beavers, D.D.Joseph : Boundary conditions at a naturally permeable wall. J. Fluid Mech., Vol 30, (1967) 197-207.
[7] V.K.Stokes, Couple Stresses in Fluids, Phys. Fluids., Vol 9,(1966) 1709-1715.
[8] V.K.Stokes, Theories of Fluids with Microstructure, Springer-Verlag, Berlin 1984.
[9] S.K.Lakshmana Rao and T.K.V.Iyengar, Analytical and computational studies in couple stress fluid flows, U.G.C. Research project C-8-4/82 SR III, (1985)
[10] L.M.Srivastava,Flow of couple stresss fluid through stenotic blood vessels, J.Bio Mech., Vol 18, 479-485 (1985)
[11] L.M.Srivastava, Perstaltic transport of a couple stresss fluid, Rheo.Acta, Vol 25, 638-641 (1986).
[12] N.B.Naduvinamani, P.S.Hiremath and G.Gurubasavaraj : Squeeze film lubrication of a short porous journal bearing with couple stress fluids, Tribo.Inter.,Vol 34, 739-747 (2001).
[13] N.B.Naduvinamani, P.S.Hiremath and G.Gurubasavaraj : Surface roughness effects in a short porous journal bearing with couple stress fluid, Fluid Dyn. Res.,Vol 31, 333-354 (2002).
[14] N.B.Naduvinamani,Syeda Taseem Fathima and P.S.Hiremath: Effects of surface roughness on characteristics of couple stress squeeze film between anisotropic porous rectangular plates, Fluid Dyn. Res., Vol 32, 217-231 (2003).
[15] M.Devakar and T.K.V.Iyengar, Stoke's problems for an incompressible couple stress fluid, Nonlinear Analysis: Modeling and Control, Vol 1, 181-190 (2008).
[16] M.Devakar and T.K.V.Iyengar, Runup flow a couple stress fluid between parallel plates , Nonlinear Analysis: Modeling and Control, Vol 15, 29-37 (2010).
[17] T.S.L.Radhika and T.K.V.Iyengar, Stokes flow of an incompressible couple stress fluid past a porous spherical shell, Proceedings of International Multi conference of Engineers and Computer Scientists, Vol 3, 1634-1639 (2010)